

sults (Fig. 2 and 3) with the pure chromium data (Fig. 1), that the electrical resistivity in the paramagnetic region rises as molybdenum is added while the thermal resistivity falls. This takes place in such a way that the magnitude of L falls quite rapidly. This unusual behavior, which also occurs in the antiferromagnetic region, can be completely understood in terms of energy-dependent band-structure effects which modify the basic electronic thermal conductivity of chromium and its alloys, and it will be explained in full elsewhere.

We wish to thank Professor S. Arajs, Clarkson College, Potsdam, New York, for the loan of the Cr:Mo samples, and the National Research Council of Canada for a grant in aid of this research.

¹G. T. Meaden, K. V. Rao, and H. Y. Loo, Phys. Rev. Lett. **23**, 475 (1969).

²S. Arajs, J. Appl. Phys. **39**, 673 (1968).

³G. T. Meaden, K. V. Rao, K. T. Tee, and H. Y. Loo, in Proceedings of the Conference on Dynamical Aspects of Critical Phenomena, Fordham Univ., New York, 1970 (to be published).

⁴W. J. Nellis and S. Legvold, Phys. Rev. **180**, 581 (1969) (thermal-conductivity peak at T_c of holmium).

⁵D. W. Boys and S. Legvold, Phys. Rev. **174**, 377

(1968) (5% Lorenz-number peak at T_c of dysprosium; thermal-conductivity extrema at T_c of erbium).

⁶S. Arajs and G. R. Dunmyre, Z. Naturforsch. **21a**, 1856 (1966) (thermal-conductivity extrema at T_N of samarium).

⁷L. R. Edwards and S. Legvold, Phys. Rev. **176**, 753 (1968) (thermal-conductivity extrema at T_N of thulium).

⁸J. P. Moore, R. K. Williams, and D. L. McElroy, Phys. Rev. Lett. **24**, 587 (1970).

⁹M. J. Laubitz and T. Matsumara, Phys. Rev. Lett. **24**, 727 (1970).

¹⁰H. Y. Loo, thesis, Dalhousie University, 1969 (unpublished).

¹¹R. W. Powell, C. Y. Ho, and P. E. Liley, *Thermal Conductivity of Selected Materials*, U. S. National Bureau of Standards National Standard Reference Data Series - 8 (U. S. G. P. O., Washington, D. C., 1966). (Our silver results, for instance, at 300 K differed by only -0.3% from the recommended value of $4.27 \text{ W cm}^{-1} \text{ K}^{-1}$ of Powell *et al.*)

¹²M. J. Laubitz, Can. J. Phys. **47**, 2633 (1969).

¹³J. P. Moore, R. K. Williams, and D. L. McElroy, in *Thermal Conductivity, Proceedings of the Seventh International Conference, Gaithersburg, Maryland, November 1967*, edited by D. R. Flynn and B. A. Peavy, Jr., U. S. National Bureau of Standards Special Publication No. 302 (U. S. G. P. O., Washington, D. C., 1968), pp. 297-310.

¹⁴If the size of the electrical-resistivity anomaly is also determined in this way, it is found to be 1.2% for our previous sample and 1.6% after annealing.

LATTICE MODE DEGENERACY IN MoS_2 AND OTHER LAYER COMPOUNDS

J. L. Verble and T. J. Wieting*

Naval Research Laboratory, Washington, D. C. 20390

(Received 29 June 1970)

The observed degeneracy of mutually exclusive infrared- and Raman-active modes in MoS_2 is traced by means of group theory to the weak van der Waals interaction between layers.

We have recently carried out an experimental investigation¹ of the long-wavelength optical phonons in the hexagonal layer compound² MoS_2 (molybdenite). The infrared-active mode for $E \perp c$ has been observed to be degenerate with one of the Raman-active modes in the basal plane. Since MoS_2 possesses a center of inversion, the infrared- and Raman-active modes must be mutually exclusive. This is the first time that mutually exclusive modes in a layer compound have been observed to be degenerate. We shall show in this Letter that the observed degeneracy is not accidental, but is traceable by means of group theory to the weak van der Waals interaction between the layers. In addition, we predict that three optically inactive

phonons will be degenerate with three optically active phonons. We further predict that mode degeneracy will prove to be characteristic of all layer compounds with more than one layer in the primitive unit cell.

Hexagonal MoS_2 , which belongs³ to the space group D_{6h} ($P6_3/mmc$),⁴ contains two molecular units and therefore six atoms within the primitive unit cell. Molybdenum and sulfur atoms are arranged in sheets parallel to the base of the hexagonal unit cell. One layer in the structure is composed of single sheets of sulfur atoms on both sides of a molybdenum sheet. For the $2H$ polytype of MoS_2 , the repeat distance along the c axis includes two of these layers. The short-range forces between atoms within a layer are

Table I. Long-wavelength lattice modes of MoS₂. The frequencies in parentheses are predicted from arguments presented in the text.

A	B	C	D	E	F
Irreducible Representations	Transformation Properties	Activity	Polarization of Vibration	Type of Ions Involved	Frequency (cm ⁻¹)
A _{2u}	T _z	Acoustical	c-axis	Mo + S	
E _{1u}	(T _x , T _y)	Acoustical	basal plane	Mo + S	
A _{2u}	T _z	IR (E ∥ c)	c-axis	Mo + S	466±1
B _{2g} ¹		Inactive	c-axis	Mo + S	(466)
E _{1u}	(T _x , T _y)	IR (E ⊥ c)	basal plane	Mo + S	384±1
E _{2g} ¹	(α _{xx} - α _{yy} , α _{xy})	Raman	basal plane	Mo + S	383±1
A _{1g}	(α _{xx} + α _{yy} , α _{zz})	Raman	c-axis	S	409±1
B _{1u}		Inactive	c-axis	S	(409)
E _{1g}	(α _{yz} , α _{zx})	Raman	basal plane	S	519±1
E _{2u}		Inactive	basal plane	S	(519)
B _{2g} ²		Inactive	c-axis	Mo + S	(low frequency)
E _{2g} ²	(α _{xx} - α _{yy} , α _{xy})	Raman	basal plane	Mo + S	(low frequency)

strong by comparison with the van der Waals forces between layers. This accounts for the extreme ease with which the crystal may be cleaved along the basal plane.

A group-theoretical analysis⁴ of lattice vibrations at the Γ point in the hexagonal Brillouin zone has been performed. The decomposition into irreducible representations is as follows:

$$\Gamma = A_{1g} \oplus 2A_{2u} \oplus B_{1u} \oplus 2B_{2g} \oplus E_{1g} \oplus 2E_{1u} \oplus E_{2u} \oplus 2E_{2g}.$$

The transformation properties of these representations⁵ are given in column B of Table I. Acoustical modes and infrared-active optical modes must transform as either T_x , T_y , or T_z and must be antisymmetric under inversion. This implies that the three acoustical vibrations consist of one mode of A_{2u} symmetry and two degenerate modes of E_{1u} symmetry. Similarly, two infrared-active modes are expected, one for $E \parallel c$ of A_{2u} symmetry and a degenerate pair for $E \perp c$ of E_{1u} symmetry. Table I also indicates that there are four Raman-active modes, namely one A_{1g} , one E_{1g} , and two E_{2g} . The polarization selection rules for exciting each of these can be determined from the transformation properties of the components of the polarizability tensor listed in column B of Table I.

The molybdenum atoms in MoS₂ occupy sites of D_{3h} symmetry, whereas the sulfur atoms are at sites of C_{3v} symmetry. The point group at each atomic site is a subgroup of the factor group of the crystal; therefore, the irreducible representations of the site groups can be correlated with those of the factor group.⁵ The correlation among representations for MoS₂ is presented in the correlation chart⁶ of Fig. 1. Since there are no rotational modes in MoS₂, only those representations which transform as T_x , T_y , or T_z are

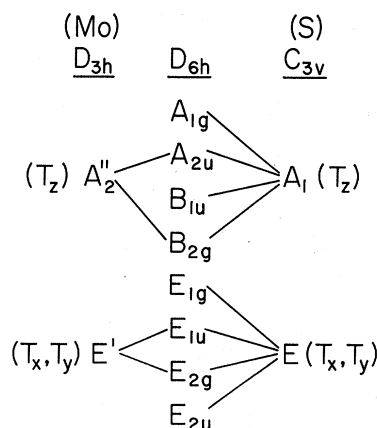


FIG. 1. Correlation chart relating the irreducible representations of the site groups D_{3h} and C_{3v} to those of the factor group D_{6h} .

considered for each site group. From the correlation chart we can determine which atoms move in each normal vibration and whether this motion is in the basal plane or along the c axis. This information is summarized in columns D and E of Table I.

The frequencies of the optically active modes have been obtained by measuring the infrared reflectivity and Raman scattering from natural specimens⁷ of MoS_2 . For $E \perp c$ one strong Reststrahl band was observed as expected. A TO mode frequency of 384 cm^{-1} has been assigned to this band by fitting an oscillator model to the reflectivity. Similarly, for $E \parallel c$ a strong Reststrahl band appeared which had a TO frequency of 466 cm^{-1} . Three Raman modes have been observed using back-scatter geometry, an argon-ion laser, and a double monochromator. The observed phonon frequencies are given in column F of Table I, and it should be noted that the E_{2g}^1 Raman-active mode is essentially degenerate with the E_{1u} infrared-active mode.

The near degeneracy of the E_{1u} and E_{2g}^1 modes can be understood by comparing the vibrational motions of the atoms in adjacent layers. In Fig. 2 we show the atomic displacements as viewed along a $[1000]$ axis⁸ of the crystal. Both of these modes are seen to involve motions of molybdenum and sulfur atoms in the basal plane. The significant difference between them, however, is that one is antisymmetric and the other symmetric with respect to inversion. Since there is an inversion center half-way between the sulfur atoms on either side of the interlayer gap, it is clear from Fig. 2 that the E_{2g}^1 mode differs from the E_{1u} mode only by an interlayer phase shift of 180° . Thus, it follows that for weak layer-layer

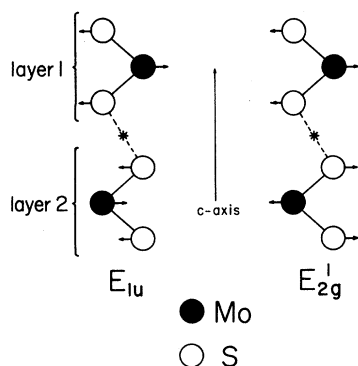


FIG. 2. Displacements of atoms in the unit cell for the E_{1u} and E_{2g}^1 modes as viewed along a $[1000]$ axis of the crystal. The asterisk denotes an inversion center.

interactions the vibrational frequencies of these two modes should be nearly the same. This is what we have observed experimentally. By considering diagrams similar to Fig. 2 for the remaining vibrations, we expect the inactive modes B_{2g}^1 , B_{1u} , and E_{2u} to be nearly degenerate with the active modes A_{2u} , A_{1g} , and E_{1g} , respectively. The predicted frequencies of the inactive modes are given in parentheses in Table I.

The B_{2g}^2 and E_{2g}^2 modes can be considered as "quasiacoustical"; that is, all three atoms within a layer vibrate in phase, but atoms in adjacent layers are 180° out of phase. Since the only restoring force for these vibrations is due to the layer-layer interaction, these modes are expected to have very low frequencies. As a result, we have not as yet observed the E_{2g}^2 Raman mode.

Our explanation of the degenerate modes in MoS_2 implies that the normal vibrations of the $2H$ polytype reduce to those of a single layer. Thus the four independent frequencies given in column F of Table I (384 , 409 , 466 , and 519 cm^{-1}) are also the optical frequencies of a single layer. Other polytypes of MoS_2 , such as the three-layered rhombohedral form ($3R$), should also have the same basic set of normal-mode frequencies. Varying the stacking sequence, so that the unit cell contains two or more layers, does not affect the phonon energies but simply creates "quasiacoustical" modes. If in addition the crystal symmetry is changed, the activity of the modes will also be altered. We expect these conclusions to apply to all layer compounds⁹ in which the primitive unit cell contains more than one layer. Since polytype formation is common in layer compounds, a large number of them should show mode degeneracy similar to that of MoS_2 .

The authors are indebted to Professor R. K. Khanna for illustrating the use of the correlation method, and to Dr. J. A. Van Vechten for helpful discussions.

*National Research Council research associate.

¹T. J. Wieting and J. L. Verble, to be published.

²For the purposes of this Letter, a layer compound is one in which all layers are structurally identical and the forces between layers are weak.

³R. W. G. Wyckoff, *Crystal Structures* (Interscience, New York, 1963), Vol. 1, p. 280.

⁴See, for example, S. H. Chen, *Phys. Rev.* **163**, (1967).

⁵E. B. Wilson, Jr., J. C. Decius, and P. C. Cross,

Molecular Vibrations (McGraw-Hill, New York, 1955), Appendix X, pp. 312-340.

⁶J. Murphy, H. H. Caspers, and R. A. Buchanan, *J. Chem. Phys.* **40**, 743 (1964); D. F. Hornig, *J. Chem. Phys.* **16**, 1063 (1948).

⁷The samples were obtained from the National Muse-

um of Natural History, Smithsonian Institution, Washington, D. C. (specimens Nos. R402, 91779, and C288).

⁸The primitive vectors in the basal plane are chosen to be perpendicular to the sides of the hexagon.

⁹J. A. Wilson and A. D. Yoffe, *Advan. Phys.* **18**, 193 (1969).

DYNAMIC PROTON POLARIZATION IN AIK AND Al(NH₄) ALUM*

Philip J. Bendt

Los Alamos Scientific Laboratory, University of California, Los Alamos, New Mexico 87544

(Received 18 June 1970)

Over 50% proton polarization has been attained in three sulfate alum crystals containing dilute Cr³⁺ ions, at 1 K and ~19.5 kG, with limited microwave power (~ $\frac{1}{4}$ W). The EPR spectra are dominated by the $(-\frac{1}{2}, \frac{1}{2})$ transition, with linewidths varying from 10 to 22 G. Al(NH₄) alum should make useful polarized proton targets because it contains 1.97 times as much hydrogen by weight as lanthanum magnesium nitrate.

In AIK(SO₄)₂·12H₂O and Al(NH₄)(SO₄)₂·12H₂O, each Al ion is surrounded by six water molecules forming a regular octahedron, with an Al-H₂O separation of about 2 Å.¹ If a small fraction (<0.5%) of the diamagnetic Al is replaced with paramagnetic Cr³⁺ ions, the paramagnetic ions are dipolar-coupled with the protons, forming a system suitable for dynamic proton polarization by the "solid effect."² We have studied the EPR spectra, relaxation times, and dynamic proton polarization in four alum crystals, along with a lanthanum magnesium nitrate (LMN) crystal for comparison.³

Though Cr³⁺ has a spin $S = \frac{3}{2}$, the EPR spectra are dominated by the $(-\frac{1}{2}, \frac{1}{2})$ transition, especially when the (111) plane is oriented perpendicular to the magnetic field H (see Fig. 1). An explanation of this was given by Bleaney,⁴ who suggested that the zero-field Stark splitting is not quite constant throughout the mixed crystal; this smears out the EPR lines, except for the $(-\frac{1}{2}, \frac{1}{2})$ transition. The theoretical EPR spectra⁵ can still be identified at 1.3 K in AIK alum, and from the spectra of crystal No. 1 we measured the zero-field splitting $2D$, obtaining 332 MHz, corresponding to 0.011 cm^{-1} . We were also able to measure the hyperfine coupling constant $|A|$ for Cr⁵³, obtaining $(1.6 \pm 0.05) \times 10^{-3} \text{ cm}^{-1}$.⁶ Details of the EPR results are contained in an article to be submitted elsewhere.

The values of p_{max} in Table I are the maximum (negative) proton polarizations we measured, and are limited by the microwave power delivered to the cavity ($190 \pm 290 \text{ mW}$).⁷ Since the allowed and "forbidden" EPR transitions are sufficiently well separated (30 G) that only the tails of the EPR lines overlap,⁸ the theory of dynamic polari-

zation in dipolar crystals by Jeffries⁹ and Borghini¹⁰ applies. The steady-state polarization is given by

$$p_s = \frac{P_0}{(1+f)(1+S_{1/2}/S)}, \quad (1)$$

where P_0 is the thermal equilibrium polarization of the ions,¹¹ f is the leakage factor, S is the EPR saturation factor, and $S_{1/2}$ is a constant which depends on the crystal properties and the magnetic field. S was determined from the cavity Q (~2000) and the microwave power. The polarization grows in with a single time constant τ ,

$$p(t) = p_s(1 - e^{-t/\tau}). \quad (2)$$

We determine both p_s and τ from polarization

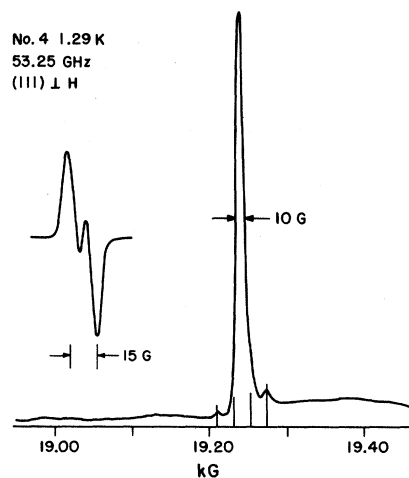


FIG. 1. The EPR spectrum of Al(NH₄) alum crystal No. 4 with the (111) planes perpendicular to the magnetic field. The positions of the four Cr⁵³ hyperfine lines are indicated. The derivative of the proton NMR line, at -44% polarization, is shown as an insert.